Biochemical Pharmacology 78 (2009) 486–494

Contents lists available at ScienceDirect

Biochemical Pharmacology

journal homepage: www.elsevier.com/locate/biochempharm

A novel δ-lactam-based histone deacetylase inhibitor, KBH-A42, induces cell cycle arrest and apoptosis in colon cancer cells

Moo Rim Kang [a,1], Jong Soon Kang [a,1], Sang-Bae Han [b], Jang Hyun Kim [a], Dong-Myung Kim [a], Kiho Lee [a], Chang Woo Lee [a], Ki Hoon Lee [a], Chul Ho Lee [c], Gyoonhee Han [c], Jong Seong Kang [d], Hwan Mook Kim [a,*], Song-Kyu Park [a,**]

[a] Bioevaluation Center, Korea Research Institute of Bioscience and Biotechnology, Yangcheong, Ochang, Cheongwon, Chungbuk, Republic of Korea
[b] College of Pharmacy, Chungbuk National University, Cheongju, Republic of Korea
[c] Department of Biotechnology, Yonsei University, Seoul, Republic of Korea
[d] College of Pharmacy, Chungnam National University, Daejoen, Republic of Korea

ARTICLE INFO

Article history:
Received 4 March 2009
Accepted 5 May 2009

Keywords:
HDAC
KBH-A42
Colon cancer
Cell cycle arrest
Apoptosis

ABSTRACT

In this study, we investigated the anti-tumor activity of KBH-A42 [*N*-hydroxy-3-(2-oxo-1-(3-phenylpropyl)-1,2,5,6-tetrahydropyridin-3-yl)propanamide], a novel synthetic histone deacetylase (HDAC) inhibitor. KBH-A42 inhibited a variety of HDAC isoforms in enzyme assays and suppressed growth of various cancer cell lines. Among the cell lines examined, colon cancer cells, including SW620, SW480 and HCT-15, were the cell types most sensitive to KBH-A42. KBH-A42 inhibition of cancer cell growth was comparable to or stronger than that of suberoylanilide hydroxamic acid (SAHA), a well-known HDAC inhibitor approved by the FDA to treat cutaneous T cell lymphomas. In SW620 cells, KBH-A42 increased the acetylation of histones, mediated cell cycle arrest (G1 arrest at low doses and G2 arrest at high doses), and induced apoptosis. The cell cycle arrest and apoptosis induced by KBH-A42 might be mediated through up-regulation of $p21^{Waf1}$ and activation of caspases, respectively. In addition, KBH-A42 inhibited SW620 tumor growth in a human tumor xenograft model. Taken together, our results indicate that KBH-A42 exerts an anti-tumor activity *in vitro* and *in vivo* and is a promising therapeutic candidate to treat human cancers.

© 2009 Elsevier Inc. All rights reserved.

1. Introduction

Histone deacetylases (HDACs) are a group of enzymes that catalyze deacetylation from lysine residues in the N-terminal tails of the core histone proteins. HDACs regulate a variety of biological processes, including proliferation, differentiation, development, and apoptosis [1]. Three classes of HDACs have been described thus far: Class I HDACs (1–3, 8, and 11) are related to the yeast RPD3 deacetylase. Class II HDACs (4–7, 9, and 10) share homology with the yeast HDAC1 deacetylase. Class III HDACs, the Sir2 family of deacetylases, are distinct from Class I and Class II HDACs and have an absolute requirement for NAD [2].

HDACs, together with the histone acetyltransferases (HATs), which catalyze the opposing reaction, participate in chromatin remodeling by modifying the acetylation status of histones. HATs mediate transcriptional activation by facilitating transcription factor binding to nucleosomal DNA [1], whereas HDACs mediate transcriptional repression by restricting the access of transcription factors [1,3]. However, recent reports suggested that HDACs also activate the transcription of several genes [2]. In addition to controlling DNA accessibility, HDACs regulate nuclear receptor functions by forming co-repressor complexes with nuclear receptors in the absence of their ligands [4]. HDACs also regulate the acetylation and function of non-histone proteins, such as p53, STAT3, estrogen receptor, and NF-κB [5].

Recently, a number of reports demonstrated that histone hypoacetylation associated with the overexpression and/or aberrant recruitment of HDAC correlated with the initiation and progression of a variety of cancers [2,6,7]. As a result of these findings, HDACs have become an attractive target for cancer therapy, and efforts in developing HDAC inhibitors as anti-cancer agents have increased. For example, suberoylanilide hydroxamic acid (SAHA, Vorinostat, Zolinza™) recently gained FDA approval for the treatment of advanced cutaneous T cell lymphoma [8]; several other HDAC inhibitors, including LAQ824, FK228, and MS-275, are currently in clinical trials [2].

* Corresponding author. Tel.: +82 43 240 6520; fax: +82 43 240 6529.
** Corresponding author. Tel.: +82 43 240 6521; fax: +82 43 240 6529.
E-mail addresses: hwanmook@kribb.re.kr (H.M. Kim), spark123@kribb.re.kr (S.-K. Park).
[1] These authors contributed equally to this work.

0006-2952/$ – see front matter © 2009 Elsevier Inc. All rights reserved.
doi:10.1016/j.bcp.2009.05.010

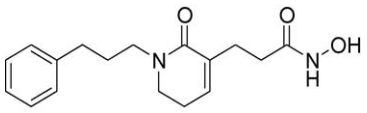

KBH-A42

Fig. 1. Chemical structure of KBH-A42.

In our search for novel HDAC inhibitors, we recently identified a series of δ-lactam-based HDAC inhibitors. We identified a lead molecule in this series that significantly inhibited HDAC activity and cancer cell growth [9–11]. Structure–activity relationship studies revealed that KBH-A42 [*N*-hydroxy-3-(2-oxo-1-(3-phenylpropyl)-1,2,5,6-tetrahydropyridin-3-yl)propanamide] was one of the most potent HDAC inhibitors among the novel δ-lactam-based compounds [10]. Unlike SAHA, which has an alkyl chain between hydroxamic acid (zinc binder) and the hydrophobic aromatic group (cap group), the zinc binder and cap group of KBH-A42 are attached through a δ-lactam ring, which mimics the hydrophobic tail group and the aliphatic chain of SAHA [10] (Fig. 1). In the present study, we examined the functional effects of KBH-A42 on the activity of various HDAC isoforms and on the growth of various types of cancer cells. In addition, we investigated the effects of KBH-A42 on cell cycle progression and apoptosis, and we explored possible molecular mechanisms that might be behind these effects. We also examined the effect of KBH-A42 on tumor growth in a human tumor xenograft model, which attested to the functional significance of these KBH-A42-mediated effects. Our results suggest that KBH-A42 might be a promising therapeutic candidate to treat human cancers.

2. Materials and methods

2.1. Chemicals, cell lines and animals

All reagents were purchased from Sigma–Aldrich (St. Louis, MO, USA) unless otherwise stated. KBH-A42 and SAHA (>99% pure) were synthesized and supplied by Dr. Gyoonhee Han at Yonsei University (Seoul, Republic of Korea). KBH-A42 was dissolved in dimethyl sulfoxide (DMSO) and freshly diluted in culture media for all *in vitro* experiments. Female BALB/c-nu mice were purchased from SLC (Hamahatsu, Japan) and maintained as described previously [12]. All animals were allowed to acclimate to the local environment for at least 1 week before use. The cell lines MDA-MB-231, HCT-15, SW480, SW620, ACHN, 786-O, NCI-H460, NCI-H23, SK-OV-3, OVCAR3, SNU-216, and NUGC-3 were cultured in RPMI 1640 medium (Gibco BRL, Grand Island, NY, USA); the U373-MG and MCF-7 cell lines were cultured in minimum essential medium (Gibco BRL); and the FHs74Int and RT4 cell lines were cultured in Dulbecco's modified Eagle's medium and McCoy's 5A medium (Gibco BRL), respectively. All media were supplemented with 10% fetal bovine serum (Hyclone, Logan, UT, USA), 2 mM L-glutamine, 100 U/ml penicillin, and 100 μg/ml streptomycin. Cells were maintained at 37 °C in 5% CO_2 humidified air.

2.2. HDAC enzyme assay

The HDAC enzymes were purchased from BPS Bioscience (San Diego, CA, USA) and the enzymatic HDAC assay was performed using a Fluorogenic HDAC Assay Kit (BPS Bioscience) according to the manufacturer's instructions. Briefly, HDAC enzymes were incubated with vehicle or various concentrations of KBH-A42 for 30 min at 37 °C in the presence of an HDAC fluorimetric substrate. The HDAC assay developer (which produces a fluorophore in reaction mixture) was added, and the fluorescence was measured using VICTOR^3 (PerkinElmer, Waltham, MA, USA) with excitation at 360 nm and emission at 460 nm. The measured activities were subtracted by the vehicle-treated control enzyme activities and IC_{50} values were calculated using GraphPad Prism (GraphPad Software, San Diego, CA, USA).

2.3. Cell proliferation assay

Cells were plated at 9×10^3 cells/well in 96-well plates, incubated overnight, and treated with KBH-A42 or SAHA for 48 h. Cell proliferation assays were performed using a Cell Proliferation Kit II (Roche Applied Science, Mannheim, Germany) according to the manufacturer's instructions. The XTT labeling mixture was prepared by mixing 50 volumes of 1 mg/ml sodium 3′-[1-(phenylaminocarbonyl)-3,4-tetrazolium]-bis(4-methoxy-6-nitro)benzene sulfonic acid hydrate with 1 volume of 0.383 mg/ml of N-methyldibenzopyrazine methyl sulfate. This XTT labeling mixture was added to the cultures and incubated for 2 h at 37 °C. Absorbance was measured at 490 nm with a reference wavelength at 650 nm.

2.4. Cell cycle analysis

Cell cycle analysis was performed using a previously described protocol [13]. Briefly, cells were plated at 3×10^6 cells/dish in 100 mm dishes, incubated overnight and synchronized by addition of serum-free media for 24 h. Next day cells were released from this block by washing and addition of fresh media and treated with the indicated concentrations of KBH-A42. After 24 h, cells were harvested and washed with PBS. After cell counting with trypan blue staining, 1×10^6 cells were pelleted and fixed in 70% ethanol at 4 °C for 1 h. Then cells were resuspended 1 ml of Krishan's buffer (0.1% sodium citrate, 0.02 mg/ml RNase A, 0.3% Triton X-100, and 50 μg/ml propidium iodide, pH 7.4) for 1 h at 4 °C. Samples were centrifuged, resuspended in 1 ml of PBS buffer, and analyzed by flow cytometry using a FACSCalibur flow cytometer (BD Bioscience, San Jose, CA, USA). Data were collected for 10,000 events. The Modfit LT program (Verity Software House; Topsham, ME, USA) was used for cell cycle modeling. For bromodeaxyuridine (BrdU) incorporation assay, cells were labeled with 10 μM BrdU (BD Pharmingen, San Diego, CA, USA) for 1 h, treated with the indicated concentration of KBH-A42 for 24 h, and then harvested. BrdU incorporation was detected by staining with FITC-conjugated anti-BrdU monoclonal antibody and the DNA was counterstained with 7-amino-actinomycin D (7-AAD). Cells were analyzed by two-dimensional flow cytometry using a FACSCalibur flow cytometer.

2.5. Western immunoblot analysis

Total protein extracts were prepared by lysing cells in RIPA buffer (50 mM Tris–Cl [pH 8.0], 5 mM EDTA, 150 mM NaCl, 1% NP-40, 0.1% SDS, and 1 mM phenylmethylsulfonyl fluoride). Subcellular fractions were prepared as follows: briefly, cell pellets were frozen at −80 °C, thawed at 4 °C, and resuspended in cytosol extraction buffer (50 mM Tris–HCl, pH 7.4, 4 mM EDTA, 2 mM EGTA, 1 mM sodium orthovanadate, 1 mM NaF, 5 μg/ml leupeptin, 5 μg/ml aprotinin, 0.2 mM phenylmethylsulfonyl fluoride, 0.5 mM DTT) at 4 °C for 10 min. Cell lysates were centrifuged at 12,000 × *g* for 30 min at 4 °C, the supernatants were collected as the cytosolic fractions. The pellets were resuspended in modified protein lysis buffer (50 mM Tris, pH 7.4, 4 mM EDTA, 150 mM NaCl, 1 mM EGTA, 5 mM EDTA, 0.5% Triton X-100, 0.25% sodium deoxycholate, 1 mM sodium orthovanadate, 1 mM NaF, 5 μg/ml leupeptin, 10 μg/ml aprotinin, 0.2 mM phenylmethylsulfonyl fluoride, 0.5 mM DTT) at 4 °C overnight and centrifuged. The particulate fraction includes membrane-organelle proteins and nucleus-associated proteins.

Protein concentrations in the lysates were determined using a Bio-Rad protein assay kit (Bio-Rad Laboratories Inc., Hercules, CA, USA) according to the manufacturer's instructions. Samples were separated on SDS-polyacrylamide gels and transferred to nitrocellulose membranes. The membranes were incubated with blocking buffer (Tris-buffered saline containing 0.2% Tween-20 and 3% nonfat dried milk) and probed with the indicated primary antibodies. After washing, membranes were probed with horseradish peroxidase-conjugated secondary antibodies. Detection was performed using an enhanced chemiluminescent protein (ECL) detection system (Amersham Biosciences, Little Chalfont, UK). The membranes were subsequently stripped and re-probed with other primary antibodies where indicated.

2.6. Cyclin-dependent kinase assay

Total protein extracts were prepared by lysing cells in lysis buffer (Cell Signaling Technology, Beverly, MA, USA). Five hundred micrograms of the protein extract were incubated with 4 μg of antibody against Cdc2 or Cdk2 (Cell Signaling Technology, Beverly, MA, USA) for 2 h at 4 °C and then incubated for 1 h with 100 μl of protein G-sepharose (Santa Cruz Biotechnology, Waltham, MA, USA). Immunocomplexes were harvested by centrifugation, washed three times with cold-PBS buffer. Each immunoprecipitate was incubated with 5 μg of histone H1 (Boehringer Ingelheim, Ingelheim, Germany), 10 mCi of [γ-^{32}P] ATP (Amersham Biosciences, Little Chalfont, UK) at 30 °C for 10 min. The histone phosphorylation was quantitated by Wallac Microbeta scintillation counter (Wallac, Turku, Finland).

2.7. Apoptosis analysis

Apoptosis analysis was performed using an Annexin V-FITC Apoptosis Detection Kit II (BD Pharmingen, San Diego, CA, USA) according to the manufacturer's instructions. Briefly, cells were plated at 3×10^6 cells/dish in 100 mm dishes, incubated overnight, and treated with the indicated concentrations of KBH-A42 for 24 h. Cells were harvested, washed with PBS, and combined with a binding buffer containing annexin V-FITC and propidium iodide. Following 15 min incubation in the dark, cells were analyzed by flow cytometry using a FACSCalibur flow cytometer.

2.8. Caspase 3/7 assay

The activities of caspases 3 and 7 were determined using a Caspase-Glo 3/7™ Assay (Promega Corporation, Madison, WI, USA) according to the manufacturer's instructions. Briefly, cells were plated at 9×10^3 cells/well in 96-well plate, incubated overnight, and treated with the indicated concentrations of KBH-A42 for 24 h. Culture supernatants were transferred to a turbid microtiter plate and mixed with equal volumes of Proluminescent caspase 3/7 substrate. Following 1 h incubation at 37 °C, luminescence was measured using a VICTOR™ Light (PerkinElmer, NJ, USA).

2.9. In vivo bioluminescence imaging of tumor growth in a human tumor xenograft model

To generate cells that stably and constitutively expressed luciferase, SW620 cells were transfected with phCMV-Luciferase FSR™ vector (Genlantis; San Diego, CA, USA) using Lipofectamine 2000 (Invitrogen, Carlsbad, CA, USA) and cultured with media containing 1 mg/ml G418 for 2 weeks. Colonies were isolated using a Pyrex® cloning cylinder and expanded for additional 2 months in media containing 500 μg/ml G418. The luciferase-expressing cell line was dubbed SW620-Luc. The SW620-Luc cells (4×10^6) were injected subcutaneously into female BALB/c-nu mice. When tumor volumes reached 50–100 mm^3, mice were randomly distributed and treated daily with vehicle, KBH-A42 (330.7 μmol [100 mg]/kg body weight, i.p.), or SAHA (330.7 μmol [87.4 mg]/kg body weight, i.p.) for 14 days. Because the HDAC inhibitor itself had the potential to increase the luminescent signal from the tumor cells by transcriptionally activating the luciferase gene [14], KBH-A42 was not administered during the last 2 days. On day 16, mice were euthanized and intravenously injected with D-luciferin (Xenogen, Hopkinton, MA, USA). Bioluminescent images were acquired using an intensified charge-coupled device (ICCD) camera in the PHOTON IMAGER™ (Biospace Lab, Paris, France).

2.10. Statistical analysis

Results are expressed as means ± S.D. A paired *t*-test was used to compare two groups, and one-way ANOVA and Dunnett's *t*-test was used for multiple comparisons using GraphPad Prism (GraphPad Software). The criterion for statistical significance was set at $p < 0.05$.

3. Results

3.1. Effect of KBH-A42 on enzyme activity of various HDAC isoforms and proliferation of human cancer cell lines

We examined the effect of KBH-A42 on enzyme activity of various HDACs: HDAC1, 2, 3, 4, 5, 6, and 8. As summarized in Table 1, KBH-A42 potently inhibited the enzyme activity of all HDACs tested, with IC_{50} values ranging from 0.022 μM (HDAC6) to 0.305 μM (HDAC5). As a reference, we examined the effect of SAHA on the activity of these HDACs. SAHA also potently suppressed the activity of all HDAC isoforms examined in our system and the IC_{50} values were comparable to that of KBH-A42 (data not shown). We next examined the effect of KBH-A42 on cell proliferation in 15 human cancer cell lines. KBH-A42 significantly inhibited cell proliferation in all cancer cell lines tested, but it did not affect the proliferation of FHs74Int cells, a normal human intestinal epithelial cell line (Table 2). Colon cancer cells, such as SW620, SW480, and HCT-15, were most sensitive to KBH-A42, whereas glioma, stomach, and bladder cancer cell lines were least sensitive. In parallel experiments, the potency and cell type specificity of SAHA were similar to those of KBH-A42 in most cases, but the effect of KBH-A42 on colon cancer cell proliferation was stronger than that of SAHA (Table 2).

3.2. Effect of KBH-A42 on histone acetylation in SW620 cells

We investigated the effect of KBH-A42 on histone acetylation in SW620 cells. As shown in Fig. 2A, KBH-A42 enhanced the acetylation of all histones examined (histone-H2A, H3, and H4). We detected histone-H3 acetylation 1 h after KBH-A42 treatment, and it increased in a time-dependent manner until 24 h. KBH-A42

Table 1
Effect of KBH-A42 on the activity of various HDAC isoforms.

Isoform	HDAC class	IC_{50} (μM), 95% confidence intervals
HDAC1	Class I	0.047 (0.020–0.108)
HDAC2	Class I	0.032 (0.023–0.044)
HDAC3	Class I	0.231 (0.161–0.332)
HDAC4	Class IIa	0.101 (0.036–0.282)
HDAC5	Class IIa	0.305 (0.184–0.503)
HDAC6	Class IIb	0.022 (0.015–0.033)
HDAC8	Class I	0.222 (0.115–0.427)

The inhibitory effect of KBH-A42 on various HDAC isoforms was analyzed by a fluorescence-based enzyme assay, as described in Section 2. The IC_{50} values were determined by nonlinear regression analysis using GraphPad Prism version 4.0 software.

Table 2
Effect of KBH-A42 and SAHA on the proliferation of various cell lines.

Cell line	Origin	GI_{50} (μM), 95% confidence interval	
		KBH-A42	SAHA
MDA-MB-231	Breast	6.49 (3.35–12.56)	6.67 (2.99–14.86)
MCF-7	Breast	3.59 (2.58–4.99)	3.03 (2.39–3.84)
HCT-15	Colon	3.51 (2.38–5.17)	5.65 (2.91–10.99)
SW480	Colon	3.11 (1.08–8.93)	6.50 (2.43–17.43)
SW620	Colon	1.70 (1.02–2.83)	3.50 (1.93–6.37)
FHs74Int	Colon	>50	>50
U373-MG	Glioma	11.00 (7.81–15.49)	6.17 (5.78–6.59)
ACHN	Kidney	5.23 (3.07–8.94)	4.32 (3.46–5.40)
786-O	Kidney	5.68 (2.15–15.03)	9.11 (6.53–12.70)
NCI-H460	Lung	4.03 (1.71–9.52)	4.43 (2.85–6.88)
NCI-H23	Lung	4.53 (2.74–7.48)	4.52 (2.51–8.14)
SK-OV-3	Ovary	4.12 (2.81–6.04)	4.16 (2.94–5.89)
OVCAR3	Ovary	3.79 (2.39–6.01)	5.45 (2.91–10.19)
SNU-216	Stomach	12.16 (6.20–23.83)	9.92 (2.77–35.57)
NUGC-3	Stomach	6.67 (5.02–8.86)	9.82 (7.53–12.82)
RT4	Bladder	32.50 (20.42–51.73)	32.48 (16.45 64.13)

Cells were plated at 9×10^3 cells/well in 96-well plates, incubated overnight, and treated with various concentrations of KBH-A42 or SAHA for 48 h. Cell proliferation was determined with an XTT assay, as described in Section 2. GI_{50} values were determined by nonlinear regression analysis using GraphPad Prism version 4.0 software.

also substantially but slowly acetylated histone-H2A and H4 (Fig. 2A); we clearly detected the acetylation of histone-H2A and H4 24 h after KBH-A42 treatment. Treatment of SW620 cells with SAHA also significantly increased acetylation of histone-H2A, H3, and H4 in a manner similar to KBH-A42 (data not shown). In addition, Fig. 2B shows that the effect of KBH-A42 on the acetylation of histone-H3 is concentration-dependent and even 0.1 μM of KBH-A42 induces histone acetylation in SW620 cells. In contrast, KBH-A42 treatment did not affect β-actin or GAPDH expression (Fig. 2A and B).

3.3. Effect of KBH-A42 on cell cycle progression, cell cycle regulatory protein expression and cyclin-dependent kinase activity in SW620 cells

Since HDAC activity is closely coupled to cell cycle progression, we investigated the effect of KBH-A42 treatment on cell cycle progression in SW620 cells. Cell cycle analysis revealed that KBH-A42 induced G1 arrest at concentrations below 1 μM and G2 arrest and cell death at concentrations above 3 μM (Fig. 3A). BrdU incorporation analysis demonstrated that cells no longer enter S phase when treated with high concentrations of KBH-A42 (3 μM or 10 μM). To investigate possible mechanisms for KBH-A42-induced cell cycle arrest and cell death, we examined whether KBH-A42 treatment altered the expression of cell cycle regulatory proteins, such as $p21^{Waf1}$, cdc2, cdk2 and cyclin A and the phosphorylation status of Rb. As shown in Fig. 4A, treatment of SW620 cells with KBH-A42 increased the expression of cyclin-dependent kinase inhibitor, $p21^{Waf1}$, in a concentration-dependent manner. Fig. 4A also shows that the level of cyclin A and phosphorylated Rb was decreased. However, KBH-A42 treatment did not affect the

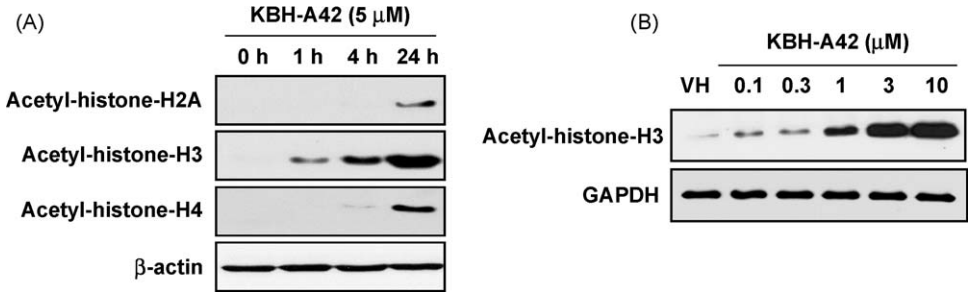

Fig. 2. Effect of KBH-A42 on histone acetylation in SW620 cells. (A) Cells were treated with KBH-A42 (5 μM) for the indicated time periods. Levels of acetylated histones and β-actin in total cell lysates were determined by Western immunoblot analysis. (B) Cells were treated with the indicated concentrations of KBH-A42 for 24 h. Acetylated histone-H3 and GAPDH in total cell lysates were determined by Western immunoblot analysis.

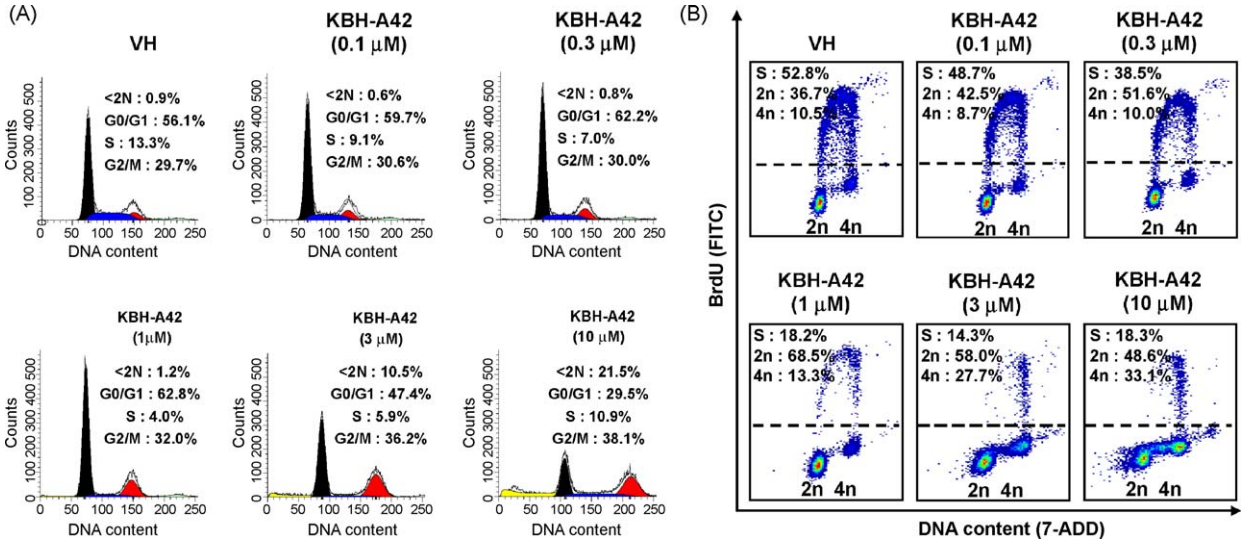

Fig. 3. Effect of KBH-A42 on cell cycle progression in SW620 cells. (A) Cells were treated with the indicated concentrations of KBH-A42 for 24 h. Cell cycle distribution was examined by flow cytometry. (B) Cells were labeled with BrdU for 1 h before cell harvested. Proliferating cells (those containing newly synthesized DNA) were labeled with BrdU and shown above the dotted line.

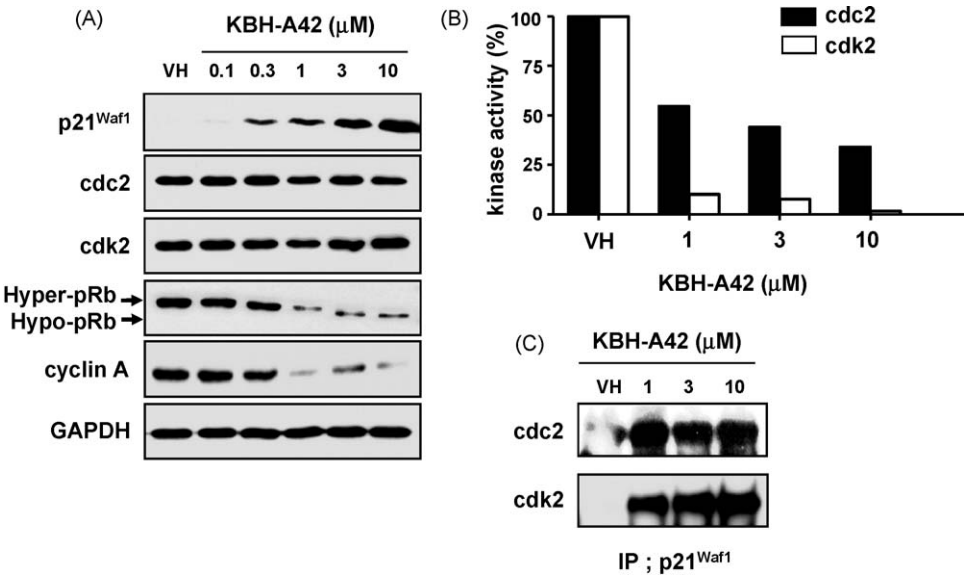

Fig. 4. Effect of KBH-A42 on the expression of cell cycle regulators. (A) Cells were treated with the indicated concentrations of KBH-A42 for 24 h. Expression levels of $p21^{Waf1}$, cdc2, cdk2, phosphorylated Rb, Cyclin A and GAPDH in total cell lysates were determined by Western immunoblot analysis. (B) After treatment with KBH-A42 for 48 h, total cell lysates were prepared and immunoprecipitated with anti-cdc2 or anti-cdk2 antibody, and kinase activity was assayed using histone-H1 as a substrate. The histone phosphorylation was quantitated by scintillation counter. (C) Total cell lysates were immunoprecipitated with anti-$p21^{Waf1}$ antibody. The amount of cdc2 and cdk2 in precipitates was determined by Western imunoblot analysis.

expression of cyclin-dependent kinases, such as cdc2 and cdk2 (Fig. 4A). Because cdc2 and cdk2 are important kinases involved in cell cycle regulation, we examined the effect of KBH-A42 on the activity of these kinases. Fig. 4B shows that the activity of cdc2 was suppressed by KBH-A42 in a concentration-dependent manner. Moreover, KBH-A42 markedly blocked the activity of cdk2 even at the lowest concentrations tested (1 μM) (Fig. 4B). To further confirm the relationship between the up-regulation of $p21^{Waf1}$ expression and down-regulation of cdc2 and cdk2 activity, we examined whether KBH-A42 induces direct association of $p21^{Waf1}$ and these kinases. As shown in Fig. 4C, the association of $p21^{Waf1}$ with cdc2 or cdk2 was almost undetectable in untreated cells. However, treatment of cells with KBH-A42 resulted in a significant increase in the binding of cdc2 and cdk2 with $p21^{Waf1}$ (Fig. 4C).

3.4. Induction of apoptosis by KBH-A42 in SW620 cells

To further investigate, we examined whether KBH-A42 induces apoptosis in SW620 cells. As shown in Fig. 5A, KBH-A42 induced apoptosis in a concentration-dependent manner; 17.7% and 30.4% of the SW620 cells were annexin V-positive after exposure 3 μM and 10 μM of KBH-A42, respectively. We also assessed whether KBH-A42 activates caspases, a key enzyme involved in apoptotic signaling cascade. As shown in Fig. 5B, KBH-A42 induced the activation of caspases 3 and 7 in SW620 cells. The activities of caspases 3 and 7 increased 5.3-fold and 8.8-fold over basal levels after treatment with 3 μM and 10 μM KBH-A42, respectively (Fig. 5B). We also confirmed that KBH-A42 treatment enhanced levels of cleaved caspase 3, the catalytically active forms of these caspases, in SW620 cells (Fig. 5D). To further elucidate the mechanism responsible for KBH-A42-induced apoptosis, we examined the effect of KBH-A42 on the expression of Bax, Bcl-2, Bcl-xL and cytochrome c, which are key molecules involved in intrinsic apoptotic pathway. As shown in Fig. 5C, KBH-A42 caused an increase in Bax expression in particulate fraction and cytochrome c release into the cytosol. Fig. 5C also shows that an anti-apoptotic protein Bcl-xL expression was down-regulated by KBH-A42 treatment. Cleavage of caspase 9 was also induced by KBH-A42 treatment in SW620 cells (Fig. 5D). Furthermore, Fig 5D also shows that KBH-A42 promoted cleavage of a well-known substrate of activated caspases, poly (ADP-ribose) polymerase (PARP), which is involved in apoptotic signaling. In addition, to determine the involvement of extrinsic apoptotic pathway in KBH-A42-induced apoptosis, we examined the effect of KBH-A42 on caspase 8 and Fas ligand in SW620 cells. Fig. 5E shows that caspase 8 activity and Fas ligand expression was not changed by KBH-A42 treatment. Treatment of SW620 cells with KBH-A42 did not affect GAPDH expression (Fig. 5B, D and E). To further confirm whether KBH-A42-induced apoptosis is caspase-dependent, we examined the effect of Z-VAD-fmk, a well-known pan-caspase inhibitor, on KBH-A42-induced apoptosis in SW620 cells. As shown in Fig. 6A, Z-VAD-fmk significantly reduced KBH-A42-induced apoptosis in SW620 cells. Consistent with the result of Fig. 6A, the inhibitory effect of KBH-A42 on the proliferation of SW620 cells was also significantly reversed by Z-VAD-fmk treatment (Fig. 6B).

3.5. Effect of KBH-A42 on the growth of SW620 tumor in nude mice

To determine whether the *in vitro* effects of KBH-A42 corresponded to anti-tumor effects *in vivo*, we examined the effect of KBH-A42 on SW620 tumor growth in a human tumor xenograft model. As shown in Fig. 7, a daily regimen of KBH-A42 injection significantly suppressed the growth of SW620 tumors. Treatment with KBH-A42 or SAHA mediated a 60% or 41% inhibition of SW620 tumor growth, respectively (Fig. 7). No significant body weight loss or normal tissue toxicity was observed in KBH-A42-treated group compared to that of vehicle-treated group (data not shown).

4. Discussion

In this study, we demonstrated that a novel δ-lactam-based HDAC inhibitor, KBH-A42, inhibited the activity of HDACs and the growth of cancer cells. Similar to SAHA or other HDAC inhibitors with hydroxamic acid moieties, KBH-A42 potently inhibited all Class I and Class II HDACs examined herein. We also confirmed the inhibitory effect of KBH-A42 on HDACs by detecting histone acetylation in cancer cells.

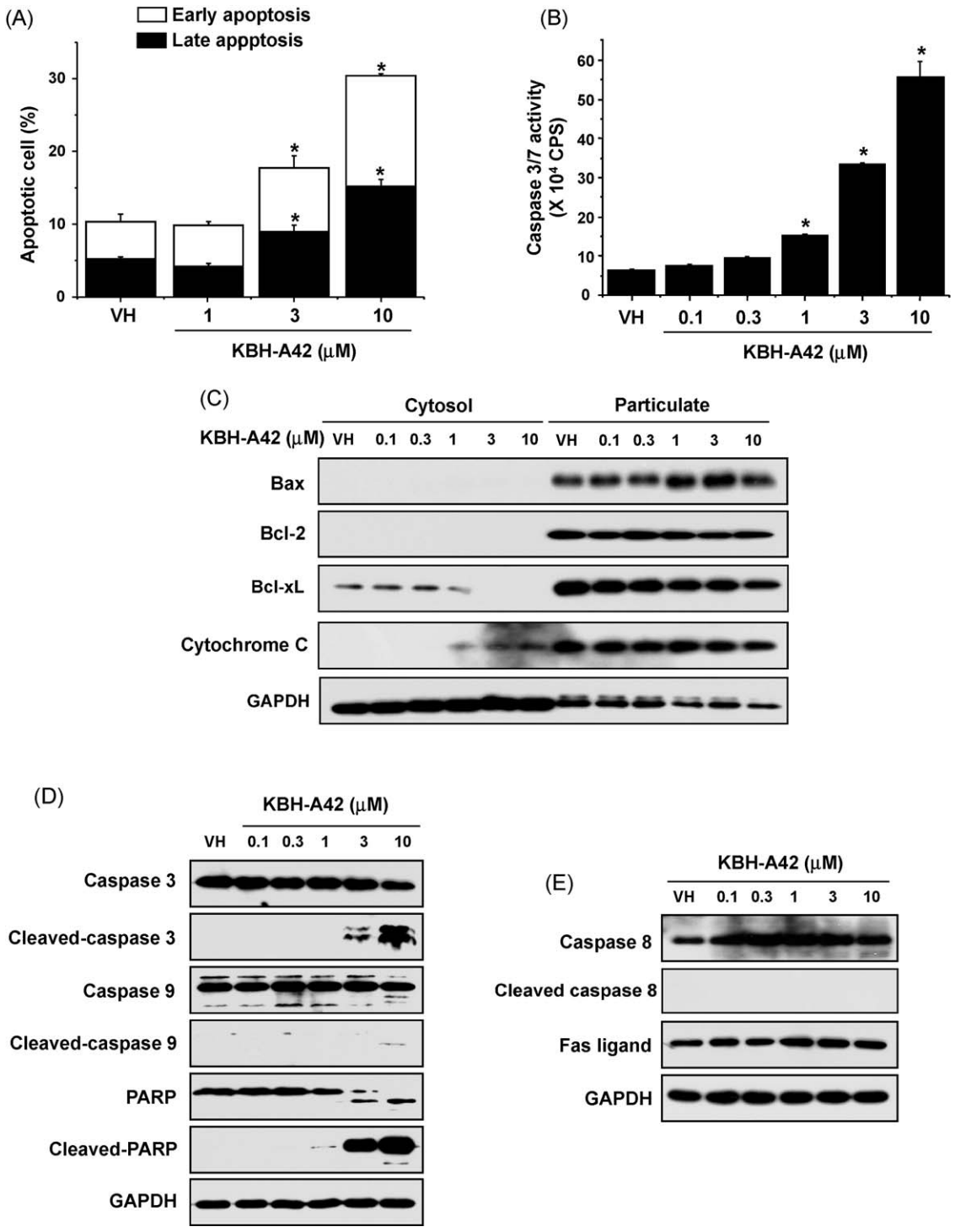

Fig. 5. Induction of apoptosis by KBH-A42 in SW620 cells. Cells were treated with the indicated concentrations of KBH-A42 for 24 h. (A) Cells were stained with propidium iodide and a FITC-conjugated antibody directed against annexin V and analyzed by flow cytometry. Results are presented as means ± S.D. of triplicate determinations. (B) Culture supernatants were collected, and the activity of caspases 3 and 7 was determined as described in Section 2. Results are presented as means ± S.D. of triplicate determinations. (C) Levels of Bax, Bcl-2, Bcl-xL, cytochrome c and GAPDH in cytosol and particulate fraction were determined by Western immunoblot analysis. (D) Levels of caspase 3, cleaved caspase 3, caspase 9, cleaved caspase 9, PARP, cleaved PARP and GAPDH in total cell lysates were determined by Western immunoblot analysis. (E) Levels of caspase 8, cleaved caspase 8, Fas ligand and GAPDH in total cell lysates were determined by Western immunoblot analysis. Significance was determined using Dunnett's *t*-test vs. the vehicle group ($^{*}p < 0.05$).

Until recently, the function of each of the HDAC isoforms was not fully understood; therefore, we have little information on the biological significance of isoform-selective HDAC inhibition in cancer therapy. Nevertheless, Karagiannis and El-Osta [15] suggested that isoform-specific HDAC inhibitors might supersede broad-spectrum HDAC inhibitors, because they could potentially regulate the expression of a more focused subset of genes. Class I HDACs, such as HDAC1 and 2, are considered to be the most clinically relevant enzymes [15], and previous reports have described HDAC1/2-specific inhibitors [16]. HDAC6 is also gaining attention as a target for anti-cancer agents, because it is the only known isoform that can deacetylate tubulin, an important target

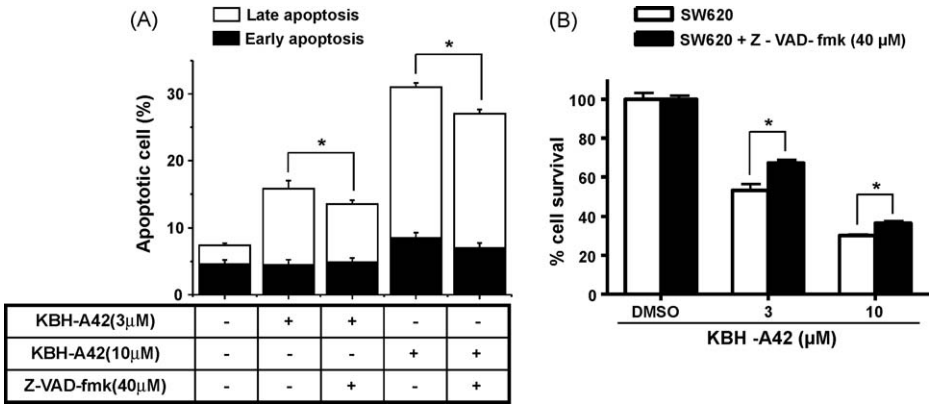

Fig. 6. Effect of caspase inhibitor on KBH-A42 induced apoptosis in SW620 cells. Cells were treated with the indicated concentrations of KBH-A42 and with or without Z-VAD-fmk (40 μM) for 24 h. (A) Cells were stained with propidium iodide and a FITC-conjugated antibody directed against annexin V and analyzed by flow cytometry. Results are presented as means ± S.D. of triplicate determinations. (B) Cell proliferation was determined by XTT assay as described in Section 2. Results are presented as means ± S.D. of triplicate determinations. Significance was determined using Dunnett's *t*-test vs. the KBH-A42 treated group ($^{*}p < 0.05$).

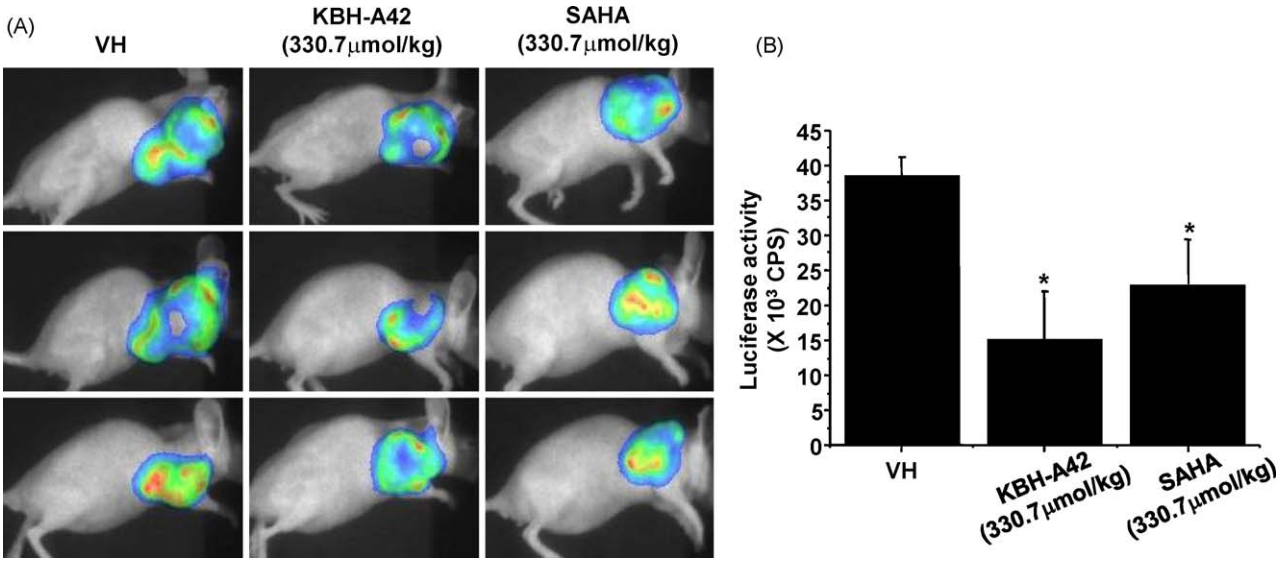

Fig. 7. Effect of KBH-A42 on SW620 tumor growth in a human tumor xenograft model. SW620-Luc cells were injected subcutaneously into female BALB/c-nu mice, and KBH-A42 (330.7 μmol/kg body weight) or SAHA (330.7 μmol/kg body weight) was administered as described in Section 2. Tumor volume was measured by bioluminescent imaging using a live animal imaging system. (A) Representative images are shown. (B) Photon counts were obtained, and results are presented as means ± S.D. of triplicate determinations. Significance was determined using Dunnett's *t*-test vs. the vehicle group ($^{*}p < 0.05$).

for cancer therapy [17]. In this study, we demonstrated that the inhibitory effect of KBH-A42 is more specific to HDAC1, 2, and 6 than to HDAC3, 4, 5, 8, and 11, suggesting that KBH-A42 might be a promising candidate for anti-cancer therapy.

We also investigated the ability of KBH-A42 to inhibit the growth of 15 cancer cell lines. Our results showed that KBH-A42 significantly suppressed the growth of all cancer cell lines tested, but that some cell types were more susceptible than others to the effect. The colon cancer cell lines were most sensitive to KBH-A42, whereas the glioma, stomach, and bladder cancer cell lines were least sensitive; this observation demonstrated a cell type-specific growth inhibitory effect of KBH-A42. Furthermore, we confirmed that KBH-A42 inhibited the growth of SW620 tumors in a human tumor xenograft model, showing that KBH-A42 exerted its anti-tumor effects both *in vitro* and *in vivo*.

Increasing evidence has revealed that HDAC inhibitors suppress cancer cell growth by inducing cell cycle arrest at G1 and/or G2 phase [18–20]. Li et al. [21] demonstrated that Trichostatin A (TSA), a natural HDAC inhibitor, inhibited the growth of bladder cancer cells through cell cycle arrest at G1 phase; TSA also mediated a G2 arrest in human melanoma cells [22]. In addition, SAHA induced G1 and/or G2 arrest in various cancer cells [23–25]. Consistent with these reports, herein we demonstrated that KBH-A42 induced cell cycle arrest in SW620 cells, suggesting that its inhibition of cancer cell growth might be mediated, at least in part, by blocking cell cycle progression. Interestingly, KBH-A42 induced G1 arrest at lower concentrations and G2 arrest at higher concentrations, revealing that KBH-A42 differentially regulated cell cycle progression depending on its concentration. In consistent with our results, it has been reported that HDAC inhibitors induce G1 arrest in most cell line and G2 arrest in a comparatively restricted number of cell lines and G2 arrest is only induced by higher doses of HDAC inhibitor than required for G1 arrest [26–28]. The exact molecular mechanism underlying this effect is not yet understood and one of the plausible explanations for this dosage effect might be that the HDACs regulating transcriptional targets that affect G2 phase are less sensitive to HDAC inhibitor. Further studies are required to clearly address this question.

The expression level of $p21^{Waf1}$, a cyclin-dependent kinase-inhibitory protein, has been implicated in the regulation of cell

cycle [29–32]. Increased expression of $p21^{Waf1}$ is associated with loss of cyclin-dependent kinase activity and dephosphorylation of Rb protein, which causes cell cycle arrest [33–35]. A variety of HDAC inhibitors are known to induce $p21^{Waf1}$ expression [28,32,26]. SAHA has been reported to induce activation of $p21^{Waf1}$ gene expression in variety of cancer cells [28,36]. Lallemand et al. [32] also reported that sodium butyrate induces $p21^{Waf1}$ expression and dephosphorylation of Rb in breast cancer cells. Consistent with these results, our data also show that KBH-A42 induces $p21^{Waf1}$ expression and hypophosphorylation of Rb in a concentration-dependent manner. We also demonstrated that the activity of cdc2 and cdk2 was suppressed by KBH-A42 treatment. Further study demonstrated that KBH-A42 induces direct interaction between $p21^{Waf1}$ and these kinases, suggesting that the cell cycle arrest induced by KBH-A42 might be mediated via $p21^{Waf1}$ induction and subsequent inhibition of cyclin-dependent kinase activity (Fig. 8).

Since HDAC inhibitors have been reported to induce apoptosis in a variety of cancer cell lines [37–39], we examined the effect of KBH-A42 on apoptosis in SW620 cells. Consistent with previous reports, KBH-A42 induced apoptosis in a dose-dependent manner, suggesting that induction of apoptosis might be another mechanism responsible for growth inhibition by KBH-A42. Caspases are a family of cysteinyl aspartate-specific proteinases that play key roles in apoptosis [40,41]. Among the 10 distinct caspases, caspases 3 and 7 are considered "executioner" caspases in the apoptotic pathway. HDAC inhibitors, such as TSA, apicidin, and sodium butyrate, induced caspase activation in cancer cells [42–44]. SAHA also induced apoptosis by activating caspases in various cancer cells [45]. In this study, we demonstrated that treatment of SW620 cells with KBH-A42 significantly increased the activity of caspases 3 and 7. This result was further supported by a Western immunoblot analysis showing that KBH-A42 treatment mediated cleavage of procaspases 3 and 7 into catalytically active effector proteins. We also demonstrated KBH-A42-induced cleavage of PARP, downstream substrates of caspases 3 and 7. Z-VAD-fmk is a broad-spectrum caspase inhibitor and it has been reported that cell death induced by SAHA was suppressed by Z-VAD-fmk treatment by blocking caspase activation [46,47]. To further confirm whether the induction of apoptosis by KBH-A42 treatment is caspase-dependent, we examined the effect of Z-VAD-fmk on KBH-A42-induced apoptosis. Our result demonstrated that pretreatment of Z-VAD-fmk significantly blocked KBH-A42-induced apoptosis in SW620 cells. In consistent with this result, KBH-A42-mediated suppression of cell proliferation was also reversed by Z-VAD-fmk treatment. $p21^{Waf1}$ is also implicated in apoptotic processes and has been reported to have both anti-apoptotic and pro-apoptotic properties. To investigate whether $p21^{Waf1}$ is involved in KBH-A42-induced apoptosis, we performed $p21^{Waf1}$ knockdown using $p21^{Waf1}$ siRNA and examined the effect of KBH-A42 on apoptosis. Our results demonstrate that $p21^{Waf1}$ knockdown had no effect on KBH-A42 induced apoptosis, suggesting that KBH-A42-induced apoptosis in SW620 cells are $p21^{Waf1}$-independent (data not shown). These results suggest that KBH-A42-induced apoptosis in SW620 cells was mediated, at least in part, by activation of caspases (Fig. 8).

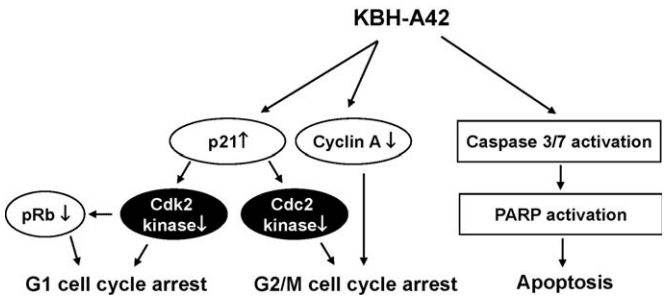

Fig. 8. Schematic diagram showing the anti-tumor effect of KBH-A42.

Two major pathways involved in apoptosis, extrinsic and intrinsic pathways, have been identified until now. Extrinsic apoptotic pathway is initiated by the engagement of cell surface death receptors with their specific ligands, which then induces caspase 8 activation [48]. In contrast, intrinsic apoptotic pathway is induced by release of cytochrome c from the mitochondria into the cytosol and activation of caspase 9, which is an initiator caspase that activates executioner caspases including caspases 3 and 7 and consequently leading to cell apoptosis [49]. Mitochondria play an important role in the regulation of cell death. Many of the pro/anti-apoptotic members of the Bcl-2 family, such as Bad and Bax also mediate their effects through the mitochondria, either by interacting with Bcl-2 and Bcl-xL [50,51] or through direct interactions with the mitochondrial membrane [52]. In the present study, we showed that KBH-A42 up-regulated Bax and down-regulated Bcl-xL. Our results also demonstrated that release of cytochrome c from the mitochondria into the cytosol and activation of caspase 9 were induced by KBH-A42 treatment, suggesting the involvement of intrinsic pathway in KBH-A42-induced apoptosis. However, extrinsic pathway was not changed by KBH-A42 treatment.

In summary, the results presented in this report demonstrated that KBH-A42 inhibits the growth of cancer cells *in vitro* and *in vivo*, and that the growth inhibitory effect of KBH-A42 might be mediated by cell cycle arrest and apoptosis via $p21^{Waf1}$ induction and caspase activation, respectively. Our results suggest that KBH-A42 might be a potential therapeutic candidate for cancer therapy.

Acknowledgements

This work was supported in part by grants from the Korea Health 21 R&D Project, Ministry of Health & Welfare, Republic of Korea (Project Number: A062254) and the KRIBB Research Initiative Program.

References

[1] Struhl K. Histone acetylation and transcriptional regulatory mechanisms. Genes Dev 1998;12:599–606.
[2] Mottet D, Castronovo V. Histone deacetylases: target enzymes for cancer therapy. Clin Exp Metastasis 2008;25(2):183–9.
[3] Wolffe AP. Transcriptional control sinful repression. Nature 1997;387:16–7.
[4] Torchia J, Glass C, Rosenfeld MG. Co-activators and co-repressors in the integration of transcriptional responses. Curr Opin Cell Biol 1998;10:373–83.
[5] Glozak MA, Sengupta N, Zhang X, Seto E. Acetylation and deacetylation of non-histone proteins. Gene 2005;363:15–23.
[6] Timmermann S, Lehrmann H, Polesskaya A, Harel-Bellan A. Histone acetylation and disease. Cell Mol Life Sci 2001;58:728–36.
[7] Lin RJ, Nagy L, Inoue S, Shao W, Miller Jr WH, Evans RM. Role of the histone deacetylase complex in acute promyelocytic leukaemia. Nature 1998; 391:811–4.
[8] Grant S, Easley C, Kirkpatrick P, Vorinostat. Nat Rev Drug Discov 2007;6:21–2.
[9] Kim HM, Lee K, Park BW, Ryu DK, Kim K, Lee CW, et al. Synthesis, enzymatic inhibition, and cancer cell growth inhibition of novel δ-lactam-based histone deacetylase (HDAC) inhibitors. Bioorg Med Chem Lett 2006;16:4068–70.
[10] Kim HM, Ryu DK, Choi Y, Park BW, Lee K, Han SB, et al. Structure–activity relationship studies of a series of novel δ-lactam-based histone deacetylase inhibitors. J Med Chem 2007;50:2737–41.
[11] Kim HM, Hong SH, Kim MS, Lee CW, Kang JS, Lee K, et al. Modification of cap group in δ-lactam-based histone deacetylase (HDAC) inhibitors. Bioorg Med Chem Lett 2007;17:6234–8.
[12] Kim HM, Lim J, Yoon YD, Ahn JM, Kang JS, Lee K, et al. Anti-tumor activity of *ex vivo* expanded cytokine-induced killer cells against human hepatocellular carcinoma. Int Immunopharmacol 2007;7:1793–801.
[13] Krishan A. Rapid flow cytofluorometric analysis of mammalian cell cycle by propidium iodide staining. J Cell Biol 1975;66:188–93.
[14] Lu YS, Kashida Y, Kulp SK, Wang YC, Wang D, Hung JH, et al. Efficacy of a novel histone deacetylase inhibitor in murine models of hepatocellular carcinoma. Hepatology 2007;46:1119–30.

[15] Karagiannis TC, El-Osta A. Will broad-spectrum histone deacetylase inhibitors be superseded by more specific compounds? Leukemia 2007;21:61–5.
[16] Park JH, Jung Y, Kim TY, Kim SG, Jong HS, Lee JW, et al. Class I histone deacetylase-selective novel synthetic inhibitors potently inhibit human tumor proliferation. Clin Cancer Res 2004;10:5271–81.
[17] Hubbert C, Guardiola A, Shao R, Kawaguchi Y, Ito A, Nixon A, et al. HDAC6 is a microtubule-associated deacetylase. Nature 2002;417:455–8.
[18] Hitomi T, Matsuzaki Y, Yokota T, Takaoka Y, Sakai T. $p15^{INK4b}$ in HDAC inhibitor-induced growth arrest. FEBS Lett 2003;554:347–50.
[19] Marks PA, Dokmanovic M. Histone deacetylase inhibitors: discovery and development as anticancer agents. Expert Opin Investig Drugs 2005; 14:1497–511.
[20] Ungerstedt JS, Sowa Y, Xu WS, Shao Y, Dokmanovic M, Perez G, et al. Role of thioredoxin in the response of normal and transformed cells to histone deacetylase inhibitors. Proc Natl Acad Sci USA 2005;102:673–8.
[21] Li GC, Zhang X, Pan TJ, Chen Z, Ye ZQ. Histone deacetylase inhibitor trichostatin A inhibits the growth of bladder cancer cells through induction of $p21^{WAF1}$ and G1 cell cycle arrest. Int J Urol 2006;13:581–6.
[22] Florenes VA, Skrede M, Jorgensen K, Nesland JM. Deacetylase inhibition in malignant melanomas: impact on cell cycle regulation and survival. Melanoma Res 2004;14:173–81.
[23] Komatsu N, Kawamata N, Takeuchi S, Yin D, Chien W, Miller CW, et al. SAHA, a HDAC inhibitor, has profound anti-growth activity against non-small cell lung cancer cells. Oncol Rep 2006;15:187–91.
[24] Kumagai T, Wakimoto N, Yin D, Gery S, Kawamata N, Takai N, et al. Histone deacetylase inhibitor, suberoylanilide hydroxamic acid (Vorinostat SAHA) profoundly inhibits the growth of human pancreatic cancer cells. Int J Cancer 2007;121:656–65.
[25] Yin D, Ong JM, Hu J, Desmond JC, Kawamata N, Konda BM, et al. Suberoylanilide hydroxamic acid, a histone deacetylase inhibitor: effects on gene expression and growth of glioma cells *in vitro* and *in vivo*. Clin Cancer Res 2007;13:1045–52.
[26] Qiu L, Burgess A, Fairlie DP, Leonard H, Parsons PG, Gabrielli BG. Histone deacetylase inhibitors trigger a G2 checkpoint in normal cells that is defective in tumor cells. Mol Biol Cell 2000;11:2069–83.
[27] Sandor V, Senderowicz A, Mertins S, Sackett D, Sausville E, Blagosklonny MV, et al. P21-dependent g1arrest with downregulation of cyclin D1 and upregulation of cyclin E by the histone deacetylase inhibitor FR901228. Br J Cancer 2000;83:817–25.
[28] Richon VM, Sandhoff TW, Rifkind RA, Marks PA. Histone deacetylase inhibitor selectively induces $p21^{WAF1}$ expression and gene-associated histone acetylation. Proc Natl Acad Sci USA 2000;97:10014–9.
[29] Richon VM, Webb Y, Merger R, Sheppard T, Jursic B, Ngo L, et al. Second generation hybrid polar compounds are potent inducers of transformed cell differentiation. Proc Natl Acad Sci USA 1996;93:5705–8.
[30] Archer SY, Meng S, Shei A, Hodin RA. $p21^{WAF1}$ is required for butyrate-mediated growth inhibition of human colon cancer cells. Proc Natl Acad Sci USA 1998;95:6791–6.
[31] Saito A, Yamashita T, Mariko Y, Nosaka Y, Tsuchiya K, Ando T, et al. A synthetic inhibitor of histone deacetylase, MS-27-275, with marked *in vivo* antitumor activity against human tumors. Proc Natl Acad Sci USA 1999; 96:4592–7.
[32] Lallemand F, Courilleau D, Buquet-Fagot C, Atfi A, Montagne MN, Mester J. Sodium butyrate induces G2 arrest in the human breast cancer cells MDA-MB-231 and renders them competent for DNA replication. Exp Cell Res 1999;247:432–40.
[33] Brugarolas J, Moberg K, Boyd SD, Taya Y, Jacks T, Lees JA. Inhibition of cyclin-dependent kinase 2 by p21 is necessary for retinoblastoma protein-mediated G_1 arrest after γ-irradiation. Proc Natl Acad Sci USA 1999;96:1002–7.
[34] Harper JW, Adami GR, Wei N, Keyomarsi K, Elledge SJ. The p21 Cdk-interacting protein Cip1 is a potent inhibitor of G1 cyclin-dependent kinases. Cell 1993;75:805–16.
[35] Hitomi M, Shu J, Agarwal M, Agarwal A, Stacey DW. $p21^{Waf1}$ inhibits the activity of cyclin dependent kinase 2 by preventing its activating phosphorylation. Oncogene 1998;17:959–69.
[36] Huang L, Sowa Y, Sakai T, Pardee AB. Activation of the $p21^{WAF1/CIP1}$ promoter independent of p53 by the histone deacetylase inhibitor suberoylanilide hydroxamic acid (SAHA) through the Sp1 sites. Oncogene 2000;19:5712–9.
[37] Louis M, Rosato RR, Brault L, Osbild S, Battaglia E, Yang XH, et al. The histone deacetylase inhibitor sodium butyrate induces breast cancer cell apoptosis through diverse cytotoxic actions including glutathione depletion and oxidative stress. Int J Oncol 2004;25:1701–11.
[38] Doi S, Soda H, Oka M, Tsurutani J, Kitazaki T, Nakamura Y, et al. The histone deacetylase inhibitor FR901228 induces caspase-dependent apoptosis via the mitochondrial pathway in small cell lung cancer cells. Mol Cancer Ther 2004;3:1397–402.
[39] Roh MS, Kim CW, Park BS, Kim GC, Jeong JH, Kwon HC, et al. Mechanism of histone deacetylase inhibitor Trichostatin A induced apoptosis in human osteosarcoma cells. Apoptosis 2004;9:583–9.
[40] Enari M, Talanian RV, Wong WW, Nagata S. Sequential activation of ICE-like and CPP32-like proteases during Fas-mediated apoptosis. Nature 1996; 380:723–6.
[41] Alnemri ES, Livingston DJ, Nicholson DW, Salvesen G, Thornberry NA, Wong WW, et al. Human ICE/CED-3 protease nomenclature. Cell 1996;87:171.
[42] Rokhlin OW, Glover RB, Guseva NV, Taghiyev AF, Kohlgraf KG, Cohen MB. Mechanisms of cell death induced by histone deacetylase inhibitors in androgen receptor-positive prostate cancer cells. Mol Cancer Res 2006;4:113–23.
[43] Park H, Im JY, Kim J, Choi WS, Kim HS. Effects of apicidin, a histone deacetylase inhibitor, on the regulation of apoptosis in H-ras-transformed breast epithelial cells. Int J Mol Med 2008;21:325–33.
[44] VanOosten RL, Earel Jr JK, Griffith TS. Histone deacetylase inhibitors enhance Ad5-TRAIL killing of TRAIL-resistant prostate tumor cells through increased caspase-2 activity. Apoptosis 2007;12:561–71.
[45] Gillenwater AM, Zhong M, Lotan R. Histone deacetylase inhibitor suberoylanilide hydroxamic acid induces apoptosis through both mitochondrial and Fas (Cd95) signaling in head and neck squamous carcinoma cells. Mol Cancer Ther 2007;6:2967–75.
[46] Huang L, Pardee AB. Suberoylanilide hydroxamic acid as a potential therapeutic agent for human breast cancer treatment. Mol Med 2000;6:849–66.
[47] Garcia-Calvo M, Peterson EP, Leiting B, Ruel R, Nicholson DW, Thornberry NA. Inhibition of human caspases by peptide-based and macromolecular inhibitors. J Biol Chem 1998;273:32608–13.
[48] Juang SH, Pan WY, Kuo CC, Liou JP, Hung YM, Chen LT, et al. A novel bis-benzylidenecyclopentanone derivative, BPR0Y007, inducing a rapid caspase activation involving upregulation of Fas (CD95/APO-1) and wild-type p53 in human oral epidermoid carcinoma cells. Biochem Pharmacol 2004;68:293–303.
[49] Tong WG, Ding XZ, Adrian TE. The mechanisms of lipoxygenase inhibitor-induced apoptosis in human breast cancer cells. Biochem Biophys Res Commun 2002;296:942–8.
[50] Assaf H, Azouri H, Pallardy M, Ochratoxin. A induces apoptosis in human lymphocytes through down regulation of Bcl-xL. Toxicol Sci 2004;79:335–44.
[51] Zhang MC, Liu HP, Demchik LL, Zhai YF, Yang DJ. LIGHT sensitizes IFN-γ-mediated apoptosis of HT-29 human carcinoma cells through both death receptor and mitochondria pathways. Cell Res 2004;14:117–24.
[52] Liu MJ, Wang Z, Li HX, Wu RC, Liu YZ, Wu QY. Mitochondrial dysfunction as an early event in the process of apoptosis induced by woodfordin I in human leukemia K562 cells. Toxicol Appl Pharmacol 2004;194:141–55.